Turbulent Flow in Square Ducts After an Expansion

Shin-ichi Nakao*
National Research Laboratory of Metrology, Ibaraki, Japan

Turbulent flow in a square duct after the expansion was investigated in detail. It was seen that the developing behavior of this flow is very different from that of the flow in straight square ducts. Especially, the secondary flow in a square duct remains very weak and does not develop far downstream, at least through $x/Dh = 40$, unlike that in a straight square duct. This can be explained by the fact that many streamwise vortices, rather than a vortex pair in the corner region, develop from the distorted vortex loop caused by the free shear of the jet-like flow at the expansion. The results also indicate that the turbulent intensities u', v', and w' do not almost change from $x/Dh = 20$, at least to $x/Dh = 40$ (where Dh is the hydraulic diameter).

I. Introduction

THE flow in square ducts with an expansion, as in a diffuser, has been investigated in detail by fluid engineers such as by Miller.[1] After an expansion, a flow separates, has large turbulent eddies, and is regulated through the mixing zone, at which point the flow has a flat and uniform velocity profile. But the studies thus far have concentrated on the flow at and just after the expansion, because the purpose was to develop a practical guide to the energy loss caused by the expansion. As a result, there have been few studies investigating such a flow far downstream. The preliminary experiments reported here investigated the flow in a square duct after expansion and showed that the flat velocity profile rapidly formed after expansion is retained far downstream. This suggests that this flow (including the formation of the secondary flow) has different developing features from those in straight square ducts. This is the motivation of the present study.

It is considered that the flow in square ducts after the expansion is, at first, a bounded jet-like flow at the expansion and then becomes a three-dimensional duct flow. The bounded rectangular jet was investigated by Foss and Jones[2] and Holdeman and Foss.[3] They discussed the secondary flow observed in this flowfield and explained the mechanism whereby the secondary flow is produced in such a flowfield. That is to say, a closed vortex loop is formed from the jet free shear at the exit of the jet. This vortex loop (stretched by the velocity gradient in the boundary layer) develops to streamwise vortices and then decays into the free boundary far downstream.

There are many studies about turbulent flow in square ducts, especially about the secondary flow generated there. The fully developed flow in square ducts was investigated in detail by Brundrett and Baines,[4] Gessner and Jones,[5] and others. Melling and Whitelaw,[6] as well as Ahmed and Brundrett,[7] investigated the developing turbulent flow in square ducts. The most complete description about the turbulent flow in square ducts was obtained in these studies. But, a clear explanation about the formation of the secondary flow has not yet been made, although there have been many studies discussing the mechanism of how the secondary flow is formed in ducts, i.e., by Perkins[8] and Gessner.[9] One idea is that some instability is produced with the growth of the boundary layer and then develops streamwise vortices. The secondary flow produced by these streamwise vortices, the magnitude of which is only about 1% of the mean velocity even in fully developed flow, strongly influences both the overall and local flowfields and is retained without decaying for long distances.

The purpose of this paper is to clarify the characteristics of the flow in a square duct after the expansion, mainly the formation of the secondary flow compared with that in a straight square duct.

II. Experimental Apparatus and Method

The schematic layout of the duct studied here is shown in Fig. 1. This system consists of two rectangular ducts (75×150 mm), six square ducts (150×150 mm), one expansion duct (expansion angle 45 deg), and one short square duct (length 200 mm). Each duct is 1.0 m long and the total length of the system (including the flow meter) is 9.4 m from the entrance. The deviation in dimensions along the duct is at most ± 1.0 mm in both the depth and the width, i.e., the maximum deviation from the average cross-sectional area is $\pm 1.3\%$. The flow system has a multiple-tube-type flow meter at the entrance, which consists of 25 total pressure tubes and a static pressure tap on each side of the walls. It is used to monitor the flow rate during the experiments from which the bulk velocity U_0 is calculated. The fluctuation of the bulk velocity is under 1%. The Reynolds number based on a bulk velocity of about 18.0 m/s and the hydraulic diameter Dh of the square duct is $Re = 1.7 \times 10^5$.

The duct marked A in Fig. 1 can be set the traversing unit, which is used to position a hot-wire probe or a total-pressure tube in a y-z plane. This unit can be positioned about ± 0.05 mm in accuracy vertically (y direction) and about ± 0.25 mm horizontally (z direction). Each duct can be removed for disassembly, so that by replacing the A duct the measurements can be made at desirable positions along the duct.

The measurements of the mean velocities and Reynolds stress components were made with a x-wire probe (DISA 55P61). The wires were made of platinum-plated tungsten, 5 μm in diameter and 1.25 mm in length. The plane of the x-array was parallel to the axial direction of ducts (x direction) and the x-wire probe was rotated as oriented in a x-y plane or a x-z plane. All of the measurements were made using DISA type 56C01 constant-temperature anemometers and the signals were linearized with DISA type 56N21 linearizers. The signals were recorded in analog form using a FM video tape recorder and subsequently digitized using a 12-bit analog-digital converter. The data reduction was done with an NEC PC9801-E microcomputer.

In the preliminary experiments, the symmetry of the mean flow was investigated by using the total pressure tube. The mean velocity was measured at three stations along the duct axis after the expansion and at 270 points in each station. It was confirmed that the degree of symmetry was very good with respect to the $z/Dh = 0.5$ plane. The asymmetry with respect to the $y/Dh = 0.5$ plane was worse, because the flow

Received April 29, 1985; revision received Sept. 14, 1985.

*Senior Research Scientist, Third Division. Member AIAA.

direction could be slightly inclined due to the asymmetry of the shape at the expansion part. Therefore, the detailed measurements with an x-wire probe were made in only a half-plane from $z/Dh=0.0$ to 0.5.

The error in the measurements consists mainly of misalignment in the placement of the hot wire in the duct, the calibration discrepancy between two wires of the x-type hot wire, and the change in the air temperature during the experiments. The total error in the present experiments was under $\pm 3\%$, except for the transverse velocities V and W. This error corresponded to over $\pm 70\%$ in the data reduction of V and W, so that they often did not satisfy the continuity equation. Thus, the results of V and W were used only as a reference because they were considered to be unreliable.

III. Results

This section describes the results of the flow in the square duct after the expansion, which are compared with the results of the straight square duct flow. The experiments of the straight square duct were carried out with using the same square ducts after the expansion shown in Fig. 1. The square duct after the expansion and the straight square duct are designated ED and SD, respectively. The position of $x/Dh=0$ in the ED is located just after the expansion as shown in Fig. 1 and in the SD at the entrance of the duct, at the flow meter.

Axial Variation of the Mean Flow

The axial development of the mean flow is shown in Fig. 2. In the SD case, the mean velocity at the center of duct U_c/U_0 increases as far as about $x/Dh=30$ with the growth of the boundary layer and then seems to reach a constant value. The figure also indicates that the turbulent intensity at the center u_c'/U_0 still is growing near $x/Dh=40$. In this case, the large values of u_c'/U_0 near the entrance, about $x/Dh=5$, can be explained by the wakes of the tubes of the flow meter.

On the other hand, in the ED case, U_c/U_0 decreases rapidly from a large value after the expansion and after gradually increasing from near $x/Dh=20$ reaches a constant value. The increase of U_c/U_0 from $x/Dh=20$ is considered to be related to the growth of the boundary layer, as in the SD case, although the central core acceleration is not observed. The turbulent intensity u_c'/U_0 decreases monotonously from the expansion part and reaches a constant value. It is interesting that this value seems to be different from that of the SD. The variations of v_c'/U_0 and w_c'/U_0 also have the same tendency. The values of U_c/U_0 and u_c'/U_0 just after the expansion, $x/Dh=0$-10, are so large that they are not indicated in this figure.

Axial Mean Velocity Contours

Figure 3 is the contour of the axial mean velocity U/U_0 at ED25, ED40, and SD38, where the number after ED or SD indicates the position of x/Dh from the expansion part of the entrance.

In these figures, the profile of ED25 is flat and the distortion of the contour lines (isovels) is not recognized. Also, the isovels of ED40 are nearly parallel to the wall in the near-wall region except in the central part of the duct. The existence of the secondary flow cannot be recognized from these figures. On the contrary, the isovels of SD38 are fairly distorted, bulging toward the corners. This means the existence of a strong secondary flow.

Axial Turbulent Intensity Profiles

The turbulent intensity u'/U_0 has a large value all over the cross section just after the expansion and is rapidly redistributed. Figure 4 is the contour of u'/U_0 at ED25, ED40, and SD38. The isovels of SD38 are remarkably distorted toward the corners, which is evidence that there is a strong secondary flow. The contours of ED25 and ED40 are very similar, including the degree of bulging toward the corner, which is rather smaller than that of SD38. The distributions along the wall bisector $y/Dh=0.5$ are shown in Fig. 5. It is seen here that the flow is almost stable from ED25 to ED40, but that flow is developing in the SD.

Transverse Turbulent Intensity Contours

Figures 6 and 7 are the contours of v'/U_0 and w'/U_0 at ED40 and SD38, respectively. In both contours, the isovels in SD38 are considerably distorted toward the corner regions, but the distortion of the isovels in ED40 are not so large. The difference noted in these figures is that the contours of the ED are symmetric, while the contours of the SD are antisymmetric profiles of each other. The distribution

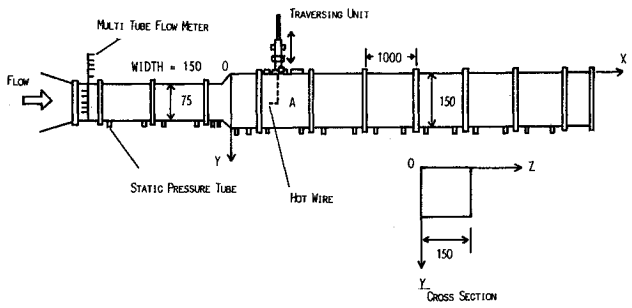

Fig. 1 Schematic layout of duct.

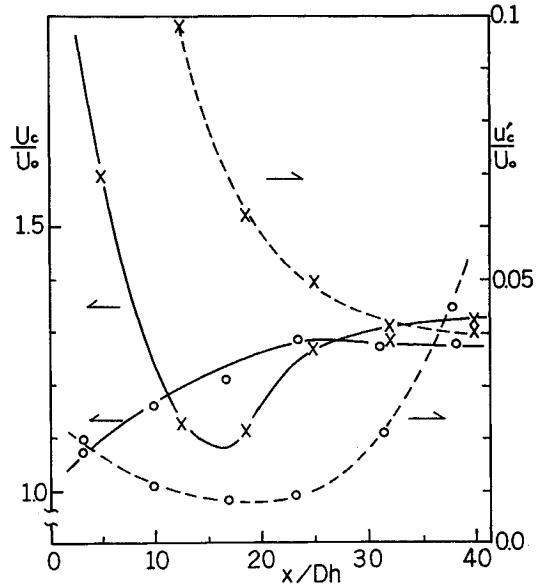

Fig. 2 Variations of mean velocity and turbulent intensity along duct axis (○ SD, × ED, —— U_c/U_0, --- u_c'/U_0).

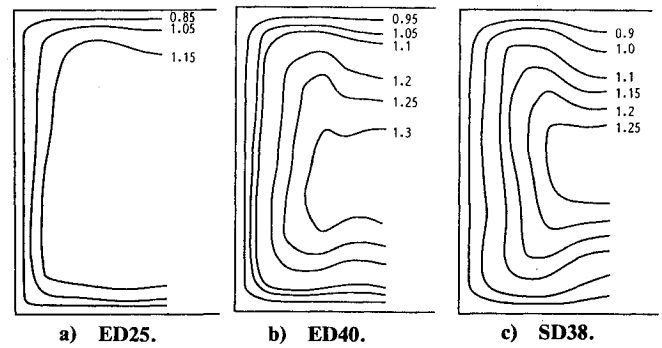

a) ED25. b) ED40. c) SD38.

Fig. 3 Contours of axial mean velocity U/U_0.

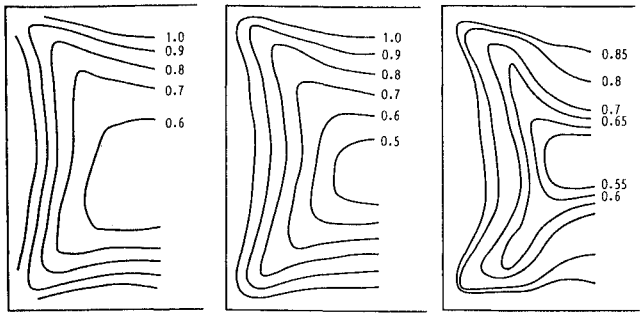

a) ED25. b) ED40. c) SD38.

Fig. 4 Contours of axial turbulent intensity $u'/U_0 \times 10$.

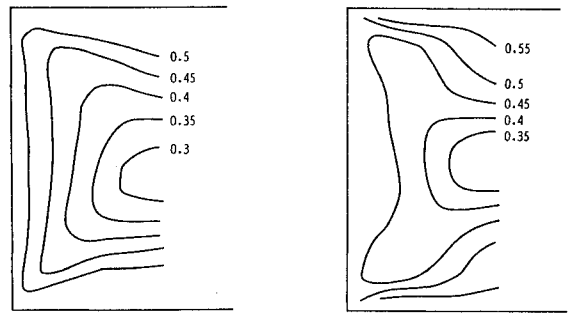

a) ED40. b) SD38.

Fig. 7 Contours of transverse turbulent intensity $w'/U_0 \times 10$.

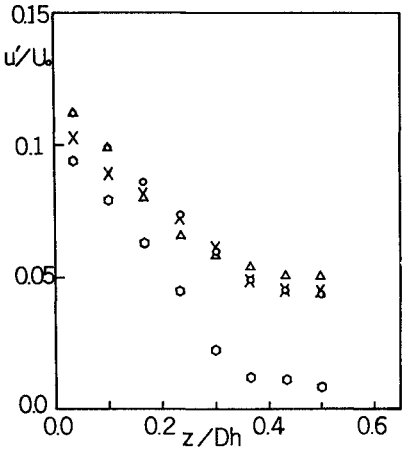

Fig. 5 Distributions of axial turbulent intensity along $y/Dh = 0.5$. (○ ED40, △ ED25, × SD38, ⬡ SD23).

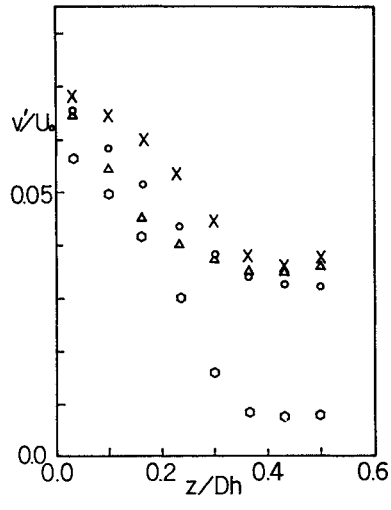

Fig. 8 Distributions of transverse turbulent intensity v'/U_0 along $y/Dh = 0.5$ (symbols as in Fig. 5).

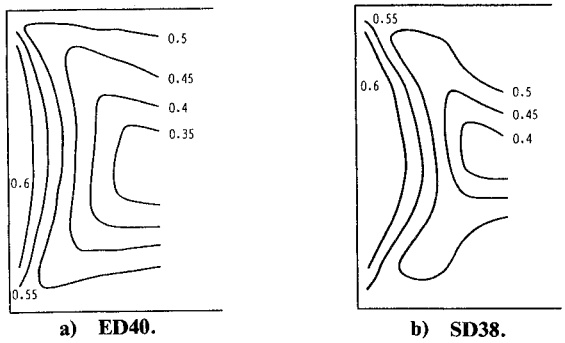

a) ED40. b) SD38.

Fig. 6 Contours of transverse turbulent intensity $v'/U_0 \times 10$.

along the wall bisector of v'/U_0 and w'/U_0 are shown in Figs. 8 and 9. The overall tendency is similar to that of u'/U_0. That is, the transverse turbulent intensities also suggest that the flow does not change very much from ED25 and ED40.

In the present experiments, the Reynolds shear stresses $\overline{uv}$ and $\overline{uw}$ were also measured. Unlike the profiles of the turbulent intensities, the Reynolds shear stresses are developing and their profiles become very similar in both the SD and ED downstream.

IV. Discussion of Results

In this section, the formation of the secondary flow in the square duct after the expansion is compared with that in the straight duct. The distortions of the contours of turbulent intensities in the ED are smaller than in the SD. These results indicate that the secondary flow in the ED is weaker than in the SD. But in the present experiments, the secondary flow could not be directly obtained, as mentioned in Sec. II. Therefore, the formation of the secondary flow will be discussed indirectly by investigating the behavior of the streamwise vorticity Ωx, because the secondary flow demonstrates the presence of streamwise vorticity Ωx. The mean streamwise vorticity equation is written as

$$\left(U\frac{\partial}{\partial x}+V\frac{\partial}{\partial y}+W\frac{\partial}{\partial z}\right)\Omega x$$
$$=\nu\left(\frac{\partial^2}{\partial x^2}+\frac{\partial^2}{\partial y^2}+\frac{\partial^2}{\partial z^2}\right)\Omega x+\Omega x\frac{\partial U}{\partial x}$$
$$+\Omega y\frac{\partial U}{\partial y}+\Omega z\frac{\partial U}{\partial z}+\left[\frac{\partial}{\partial x}\left(\frac{\partial \overline{uv}}{\partial z}-\frac{\partial \overline{uw}}{\partial y}\right)\right]\Big/P1$$
$$+\left[\frac{\partial^2}{\partial y\partial z}(\overline{v'^2}-\overline{w'^2})\right]\Big/P2+\left[\left(\frac{\partial^2}{\partial y^2}-\frac{\partial^2}{\partial z^2}\right)\overline{vw}\right]\Big/P3$$

where

$$\Omega x=\frac{\partial W}{\partial y}-\frac{\partial V}{\partial z},\quad \Omega y=\frac{\partial V}{\partial x}-\frac{\partial U}{\partial y},\quad \Omega_z=\frac{\partial U}{\partial z}-\frac{\partial W}{\partial x}$$

On the right-hand side, $P1$, $P2$, and $P3$ represent the production of streamwise vorticity by the Reynolds stress components. That is to say, the secondary flow toward the corner is generated by these terms. Empirical observation shows that $P2$ is the greatest and most effective, $P1$ is very small, and $P3$ is negligibly small. The contour of $P2$ is shown in

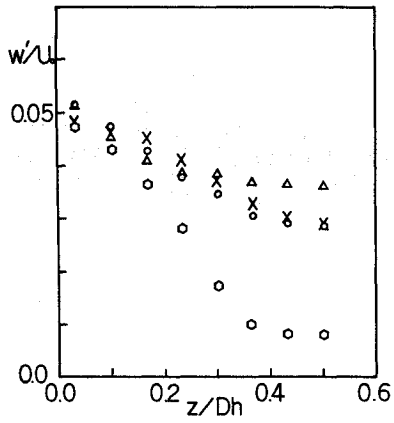

Fig. 9 Distributions of transverse turbulent intensity w'/U_0 along $y/Dh=0.5$ (symbols as in Fig. 5).

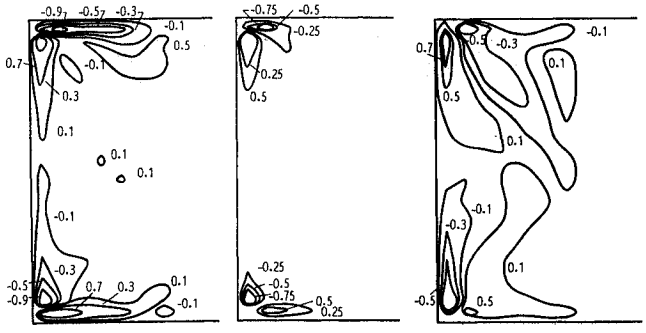

a) ED25. b) ED40. c) ED38.

Fig. 10 Contours of production term of streamwise vorticity, $\partial^2(v'^2-w'^2)/\partial x\partial y/U_0^2\times 10$.

Fig. 10. The extension of the contour in ED40 becomes smaller than in ED25 and the contour is limited to the small corner region. On the contrary, the contour of SD38 spreads over the center region, although the region of maximum production seems to be closer to the walls than the results of Brundrett and Baines.[4] The result is that the main part of the production becomes smaller downstream, which means that the streamwise vortices and the secondary flow produced by them does not develop. Conversely, it is found from Fig. 10 that the SD has a strong secondary flow. The smaller value of $P2$ in the ED is considered to be related to the profiles of v'/U_0 and w'/U_0, which were shown in Figs. 6 and 7. Although the contours of v' and w' in the SD show antisymmetric profiles, their contours at ED40 show a very similar pattern all over the cross section. Accordingly, the value of $(v'^2-w'^2)$ in the ED becomes almost zero in the wider region. The similar profiles of v'/U_0 and w'/U_0 are found in the developing flow in the SD where the secondary flow is still weak. But unlike in the ED, they become antisymmetric downstream with the development of the secondary flow.

The flow in the square duct after the expansion is considered to be a kind of bounded jet initially; hence, it already has a vortex loop just after the expansion. But unlike the case of the bounded jet, this vortex loop is entrained in the boundary layer before developing. And it is distorted by the velocity gradient in the boundary layer, resulting in many streamwise vortices. If the vortex loop changes into a pair of vortices in the corner region as in a straight square duct flow, the profiles of v' and w' will become antisymmetric, which means that $P2$ becomes larger and streamwise vortices develop. But many streamwise vortices produce the symmetric profiles of v' and w'. Therefore, the secondary flow produced by these streamwise vortices does not develop because of the smaller value of $P2$. This is the reason why the secondary flow in the square duct after the expansion is not developing and remains weak far downstream.

V. Conclusions

Detailed measurements were made of the turbulent flow in a square duct after the expansion. It was revealed that the flow has some interesting features in comparison with the flow in the straight square duct:

1) The secondary flow in this flowfield is made from many streamwise vortices along the walls, not a pair of vortices in the corner region as in a straight square duct. These streamwise vortices, which are produced from the distorted vortex loop caused by the free shear of the jet-like flow at the expansion, produce symmetric profiles of transverse turbulent intensities v' and w', resulting in the smaller amount of streamwise vorticity. Therefore, the secondary flow remains weak without developing far downstream, at least to $x/Dh=40$.

2) After the expansion, the turbulent intensities u', v', and w' change very little for a long distance, at least from $x/Dh=20$ to 40. This means that the similar profiles of v' and w' are retained in this region.

The characteristics of the flow mentioned above are considered to come from the inlet condition, which is a kind of bounded jet. So, it is considered that the flow begins to develop as a straight square duct flow after the effect of the inlet is lost, although the present results, i.e., the behavior of the turbulent intensity, do not always indicate that the effect of the inlet is lost far downstream. In any event, the present results demonstrate that the development of the secondary flow in the square duct is restrained for a long distance by the inlet conditions of jet-like flow, even if it is temporary.

References

[1]Miller, D. S., "Internal Flow Systems," *BHRA Fluid Engineering Series*, Vol. 5, 1978.

[2]Foss, J. F. and Jones, J. B., "Secondary Flow Effects in a Bounded Rectangular Jet," *Transactions of ASME, Journal of Basic Engineering*, Vol. 90, 1968, pp. 241-248.

[3]Holdeman, J. D. and Foss, J. F., "The Initiation, Development and Decay of the Secondary Flow in a Bounded Jet," *Journal of Fluids Engineering*, Vol. 97, 1975, pp. 342-352.

[4]Brundrett, E. and Baines, W. D., "The Production and Diffusion of Vorticity in Duct Flow," *Journal of Fluid Mechanics*, Vol. 19, 1964, pp. 375-394.

[5]Gessner, F. B. and Jones, J. B., "On Some Aspects of Fully Developed Turbulent Flow in Rectangular Channels," *Journal of Fluid Mechanics*, Vol. 23, 1965, pp. 689-713.

[6]Melling, A. and Whitelaw, J. H., "Turbulent Flow in a Rectangular Duct," *Journal of Fluid Mechanics*, Vol. 78, 1976, pp. 289-315.

[7]Ahmed, S. and Brundrett, E., "Turbulent Flow in Non-Circular Ducts, Part 1," *International Journal of Heat and Mass Transfer*, Vol. 14, 1971, pp. 365-375.

[8]Perkins, H. J., "The Formation of Streamwise Vorticity in Turbulent Flow," *Journal of Fluid Mechanics*, Vol. 44, 1970, pp. 721-740.

[9]Gessner, F. B., "The Origin of Secondary Flow in Turbulent Flow along a Corner," *Journal of Fluid Mechanics*, Vol. 58, 1973, pp. 1-25.